

MICROSCOPIC KINETIC MODEL
EXHIBITING CHIRAL SYMMETRY BREAKING
[Bruce Berne Symposium, ACS, Boston, Aug. 22-25, 2010]

[View 1.](#) Title, Princeton collaborators, acknowledgements

One of the more intriguing challenges presented by molecular biology is why so many of the chemical building blocks out of which living organisms are formed display an almost completely broken symmetry with respect to left and right hand geometries. In other words, why does terrestrial life exhibit a strongly preferred chirality? As emphasized in View 2 this is evident in observed molecular structures of proteins, DNA,

[View 2.](#) Motivating mysteries

carbohydrates, and other biopolymers. These observations naturally raise other underlying basic questions: (a) how did this broken geometric symmetry arise on the early earth, and (b) is the appearance of life and its subsequent evolution contingent on such broken symmetry? It also leads astrobiologists and others (c) to wonder about the presence of opposite chirality elsewhere in the universe, including that possibly present in extraterrestrial life forms.

It may never be possible to attain definitive answers to these questions. However it is feasible and a clear scientific obligation to explore possible physical and chemical scenarios that conceivably could have produced the broken symmetry observed on our planet. In that spirit the purpose of this short lecture is to propose and to describe properties of one model as representing one possible contributor to the present terrestrial situation.

With one exception (glycine) the 20 standard amino acids serving as the building blocks for proteins are individually chiral. With rare exceptions they exhibit only one mirror-image form in terrestrial biology. The following View 3 illustrates this for the

[View 3.](#) D and L forms of alanine

specific case of alanine. The rigid tetrahedral bonding at the central " α " carbon atom produces two distinct arrangements of the four attached groups. Biologically occurring alanine, either by itself or as a subunit in proteins, exhibits the so-called "L" form indicated on the left. Compared to $k_B T$ under normal biological conditions, the potential energy barrier for chiral inversion is sufficiently high that the separate D and L forms can be considered as distinguishable species.

The refereed published literature presents several possible mechanisms for emergence of a dominating chirality. The next View 4 lists five of these. The first entry involving

[View 4.](#) Possible mechanisms

weak interactions has been proposed but is almost certainly many orders of magnitude too weak to be a serious contender. Scenarios (2), (3), and (4) are much more plausible possibilities. My Princeton colleagues and I have created and numerically investigated another possibility, a simple

but geometrically explicit molecular-level model illustrating the operation of the last of the five listed scenarios. Its details will now be described.

The following View 5 presents the basic ingredients in our "minimalist" model. This

[View 5.](#) Two-dimensional lattice model

involves a two-dimensional square lattice on which two achiral reactants A and B—B reside. The former occupies one lattice site, while the latter occupies two nearest-neighbor sites. Multiple occupancy at any lattice site is forbidden. Empty sites can be interpreted as occupied by inert solvents, which for present purposes need not be explicitly indicated. The achiral reactants are capable of irreversibly forming a rigid covalent bond so as to produce a bent three-site molecule, which can permanently be in either one of two chiral forms. The reactant and product particles are kinetically allowed elementary diffusive jumps, via translational and/or rotational transitions. The implicit solvent particles are assumed as to move out of the way of such diffusive jumps as necessary. Time evolution of the many-body system is examined by Monte Carlo simulation. It should be emphasized that the model's two-dimensionality is a convenient tactic invoked in the interest of ease of visualization, but is not a fundamental restriction.

Three kinds of reaction rates are specified for the model. The first, illustrated explicitly in View 6, involves the just-mentioned irreversible covalent bond

[View 6.](#) Irreversible covalent bond formation to produce one or the other bent 3-site molecule.

formation from an A + B—B contact cluster in one of the two possible bent conformations. The temperature-dependent chemical rate constant for this process is assigned as $\exp(-\beta E_a)$, $\beta = 1/k_B T$, $E_a > 0$, for any neighboring-site composition, with one fundamental exception. This fundamental exception involves an autocatalytic cluster arrangement, wherein an initially unbonded A + B—B combination resides in the cleft of an already-formed chiral product molecule, which then catalyzes production of its own kind. This autocatalytic process is illustrated in View 7, for which the irreversible

[View 7.](#) Autocatalytic enhancement of 3-site product in the cleft of one of its own chiral kind.

chemical reaction rate is assigned to be $\exp(-\beta E_a^{cat})$, where $E_a > E_a^{cat} \geq 0$.

Finally we introduce an inhibition mechanism that has the capacity to discriminate kinetically in favor of a dominant enantiomorph, presuming that such a population bias has already arisen for some reason. As View 8 shows, this involves a reversible cluster

[View 8.](#) Reversible cluster binding of a pair of opposite-chirality product molecules, residing simultaneously in each others' clefts.

binding of two opposite-chirality product molecules in an arrangement that has each one occupying the cleft of the other. While in this arrangement, neither participant is available to catalyze formation of its own enantiomer, but this imposes fractionally a greater kinetic penalty on the minority enantiomeric population. No potential energy barrier is postulated for the formation of

this 6-site complex, but a dissociation rate is assigned as $\exp(-\beta|\epsilon|D)$, $|\epsilon| \geq 0$. In other words, the participating opposite-chirality particles experience a binding energy of $\epsilon < 0$ when they come together in this kind of cluster configuration.

It should be noted in passing that despite the presence of one of each enantiomer in such a bound cluster, the result is in fact chiral. There are two structures possible for such a racemic two-trimer cluster, and these are mirror images of one another. However this geometric distinction does not in itself have any implication for the overall chiral symmetry breaking that the minimal model has been constructed to investigate.

In order to identify intrinsic spontaneous chiral symmetry breaking for this model, it is absolutely important to guarantee that initial Monte Carlo configurations do not involve any geometric bias toward one enantiomer vs. the other. View 9 provides an example of

[View 9](#). Bias-free initial configuration, equal numbers of reactants A and B—B, $\phi = 1/3$.

a starting arrangement, with equal numbers of A and B—B reactants, that by virtue of its reflection symmetries is intrinsically unbiased. The example shown can be replicated in both basic directions for larger-system initial condition use. The coverage fraction for this example is $\phi = 1/3$, but other bias-free initial conditions can easily be constructed for different ϕ values.

The following View 10 provides some further technical details about the Monte Carlo

[View 10](#). Monte Carlo simulation details

simulations that have been performed with this two-dimensional "minimalist" model. These details include system sizes (with periodic boundary conditions), random visiting of particles with random choice of either diffusion or reaction (if either is possible), and the reckoning of advancing clock time. As the A and B—B reactants are irreversibly consumed, the MC simulation becomes less and less informative so far as the chiral-symmetry-breaking phenomenon is concerned, because the Monte Carlo moves become dominated by diffusive (non-reactive) transitions. Therefore any one simulation is halted when the mole fraction of A (equivalently of B—B) declines from its initial value $x_A(t=0) = 0.50$ to $x_A = 0.10$, at which point the presence of spontaneous symmetry breaking will virtually always have become clear.

For any given choice of transition state energies E_a , E_a^{cat} , and of dimer energy ϵ , as well as of the temperature $T = 1/(k_B T)$, the objective is to determine the distribution of enantiomer mole fractions f among product particles, which can informally be denoted by "D" and "L":

$$f = \frac{(D)}{(D) + (L)}, \quad 0 \leq f \leq 1.$$

To do this, a large number (10^4 to 10^5) of nominally equivalent MC runs for each choice of rate constants were performed, differing only by the random number generator output that underlies the successive MC transitions -- that is, the coupling to a temperature-controlled "heat bath".

As an introductory test of the model and of the MC procedure, a set of runs was carried out to observe ϕ dependence of simple diffusion rates in the absence of chemical reaction and of

inhibitory cluster binding. Specifically this amounts to setting $E_a = E_a^{cat} = +\infty$, and $\varepsilon = 0$. Translational diffusion rates were determined by the long-time asymptotes of mean-square positional displacement. View 11 presents a set of

[View 11](#). Translational diffusion constants vs. ϕ for non-reacting systems.

results showing how the diffusion constants vary with respect to covering fraction ϕ , relative to their values at infinite dilution ($\phi = 0$). The cases shown include pure A, pure B—B, and pure racemic bent product particles (C), as well as equimolar A + B—B and A + B—B + C(racemic) mixtures. The results clearly indicate non-trivial kinetic interference effects, though for the two reactant species these remain modest in magnitude up to $\phi \approx 0.80$, and so do not present a clear case that chiral symmetry breaking would be qualitatively influenced by packing effects over the density range considered.

Returning to the reactive cases that are the principal object of interest, View 12 shows

[View 12](#). Distributions of enantiomer fractions at termination of the MC run sets. The conditions involved are $\phi = 1/3$, $E_a^{cat} / E_a = 0$, and $\varepsilon / E_a = 0$. Results are illustrated for four reduced temperatures, and $\phi = 1/3$.

four probability distributions $P(f)$ at different temperatures for the final fractions of one of the chiral enantiomers. These distributions, as expected, are symmetric about the racemic point $f = 1/2$. The results shown are all from 36×36 periodic boundary condition systems with $\phi = 1/3$, repeated 10^5 times, and binned. [Note that with these system size and ϕ choices the initial numbers of **A** and of **B—B** reactants are 144; for 90×90 systems the initial numbers of reactants would be 900.] The graph shows results with strong catalysis but no specific inhibitory product pairing:

$$E_a^{cat} / E_a = 0, \quad \varepsilon / E_a = 0,$$

and with four reduced temperatures:

solid black: $\beta E_a = 10$

solid red: $\beta E_a = 8$

solid blue: $\beta E_a = 6$

dashed green: $\beta E_a = 4$.

Notice how lowering the temperature causes an initially single-peaked distribution of f values around the racemic value $f = 1/2$ to broaden and then become bimodal. That is, the model can exhibit spontaneous chiral symmetry breaking provided the temperature is low enough. In this respect it is analogous to the zero-external-field ferromagnetic Ising model, for which cooling from high temperature encounters a spontaneous magnetization symmetry breaking at the critical temperature. But also notice that even in the lowest temperature case ($\beta E_a = 10$, black curve), where most reactions will have been catalyzed, there is still a significant fraction of results around the racemic midpoint $f = 1/2$.

The following View 13 exhibits corresponding temperature-variable results, with the

[View 13](#). Same as View 12 conditions, except inhibition has been included with $\varepsilon/E_a = -10$.

same color scheme for four reduced temperatures, differing from the previous View 12 situation only by inclusion of a strong inhibitory clustering:

$$\varepsilon/E_a = -10$$

As might have been expected, this inhibition enhances the symmetry-breaking phenomenon, causing it to appear first at a higher temperature. Also note that at the same lowest temperature (black curve) as in the preceding View 12 the distribution $P(f)$ has now become nearly zero in the neighborhood of the racemic point $f = 1/2$. But also note that at the lowest temperature the enhanced bimodal $P(f)$ now peaks just inside the pure-enantiomorph values $f = 0.1$. This last feature stems from the fact that inhibition is not possible if only one enantiomer is present in the system.

For the purposes of interpreting data generated by the MC simulations, it is useful to have a quantitative criterion to separate cases with, and without, spontaneous chiral symmetry breaking. The following View 14 briefly describes one such criterion that we

[View 14](#). Sample skewness for enantiomeric excess.

have used. It converts the f distribution $P(f)$ to the distribution $\hat{P}(e)$ of enantiomeric excess $e = |2f - 1|$, then uses the second and third moments of that distribution to define a skewness g . At high temperature where $P(f)$ is concentrated around the racemic value $f = 1/2$, this definition yields $g > 0$; in the low-temperature symmetry-broken situation, $g < 0$. We identify the crossover value $g = 0$ as the location of the symmetry-breaking "phase transition".

Using this criterion, the top portion of View 15 shows the $g = 0$ "phase separation"

[View 15](#). Top: "Phase diagram", $g = 0$ curves for no hetero-inhibition ($\varepsilon = 0$) and for extremely strong hetero-inhibition [$\varepsilon/(E_a - E_a^{cat}) = -10^6$]. Above each curve symmetry breaking has occurred, below it has not. Bottom: fraction of reactions which are non-catalytic. In both graphs the solid circles and squares refer to 36×36 systems, the open circles and squares refer to 90×90 systems.

curves in a relative-energy-barrier, inverse-temperature plane. Curves are shown with no hetero-inhibition ($\varepsilon = 0$) and for extremely strong hetero-inhibition [$\varepsilon/(E_a - E_a^{cat}) = -10^6$]. For each curve the upper region represents symmetry breaking, below the curve it is absent. The bottom portion of View 15 indicates how inclusion of extremely strong inhibition [$\varepsilon/(E_a - E_a^{cat}) = -10^6$] can depress the fraction of chemical reactions that involve the catalytic route, simply because catalytic clefts are tied up. Although system size effects are quantitatively visible in both graphs, the qualitative trends remain for different sizes. Details aside, it is clear that the two-dimensional model clearly presents a mechanism for spontaneous chiral symmetry breaking.

Although more thorough investigations of rate constant selection and of ϕ variation are desirable, it is also worth identifying how our "minimalist" two-dimensional model might be elevated into a somewhat more realistic three-dimensional version. View 16

[View 16.](#) D=3 extension: The simple cubic lattice

indicates one way this could occur, using the simple cubic lattice as the host space. In this case the reactant particles could simply be one species, specifically dimers occupying a pair of nearest neighbor sites, and capable of chemically bonding to form rigid non-linear chiral tetramers. As indicated in View 16 the analog of the cleft-binding autocatalytic cluster would involve occupancy of all eight vertices of an elementary cube in the lattice. Chiral enantiomers can mathematically be distinguished by the sign of the scalar triple product defined by the ordered bond vectors. Inhibitory clusters comprising a pair of opposite enantiomer tetramers would occupy at most seven vertices of an elementary cube, but this structure can be continued iteratively to produce a racemic linear "polymer" that disproportionately ties up the minor-population enantiomorph (structure not shown).

Three final concluding remarks are summarized on the final View 17. First, it is

[View 17.](#) Concluding remarks

important to stress that the hydrodynamic phenomena of convection and/or mechanical stirring are not present in the "minimalist" model, although in a realistic scenario these would influence the symmetry-breaking outcome somewhat. Specifically these phenomena would likely enhance symmetry breaking in very large systems. That possibility suggests that generating continuum models incorporating chemical reactivity features similar to those already discussed, but with hydrodynamic flows possible, would be a valuable future direction. However such a continuum extension would entail many technical details and complications that could be conceptually distracting. Finally, it should be emphasized that the chemical reactions which for simplicity were treated as irreversible in our minimalist model could in principle be rendered reversible, though with slow reverse rates to preserve the symmetry breaking capacity. One novel way to incorporate an aspect of reversibility would be to postulate a catalytic "sandwich trimer": two identical enantiomers with one opposite enantiomer between them which is then catalyzed to revert to its unbonded precursor reactants. This should contribute to the chiral symmetry breaking phenomenon.

MICROSCOPIC KINETIC MODEL EXHIBITING CHIRAL SYMMETRY BREAKING

Harold W. Hatch, Pablo G. Debenedetti
Chemical Engineering Dept., Princeton

Frank H. Stillinger
Chemistry Dept., Princeton

Acknowledgement: Prof. Donna G. Blackmond, Imperial College, London,
and The Scripps Research Institute, La Jolla, CA

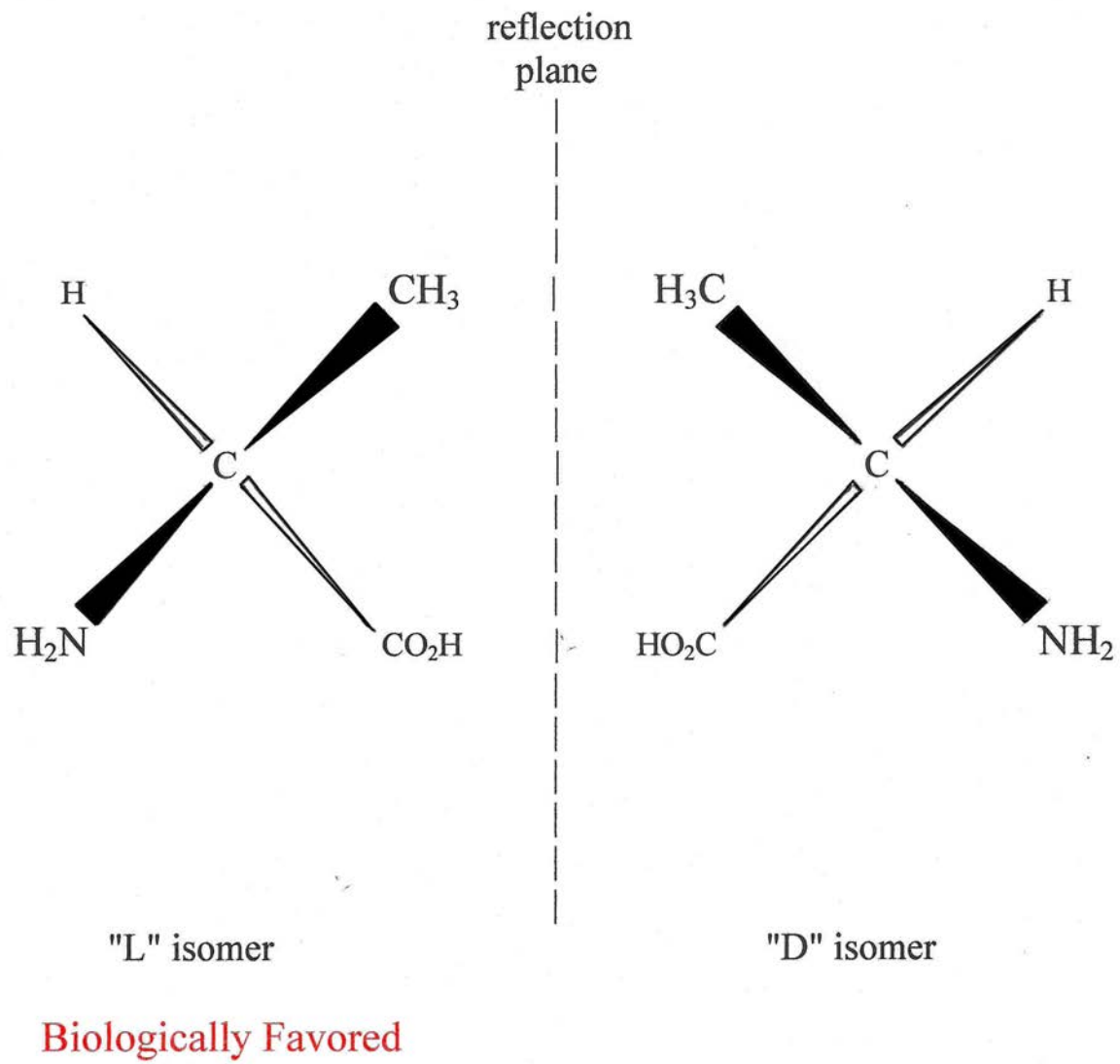
Financial Support: NSF Collaborative Research in Chemistry Grant

MOTIVATING MYSTERIES

- Biological molecules (proteins, DNA, carbohydrates, ...) occur overwhelmingly with chiral subunits that exhibit only one of the two possible mirror image forms.
- How did this broken geometric symmetry arise?
- Is the spontaneous appearance of life and its subsequent evolution possible only in such a symmetry-broken chemical environment?
- How far must one search in the universe to find C,N,O,H based life with the opposite chirality?

AMINO ACID EXAMPLE: ALANINE

BACK



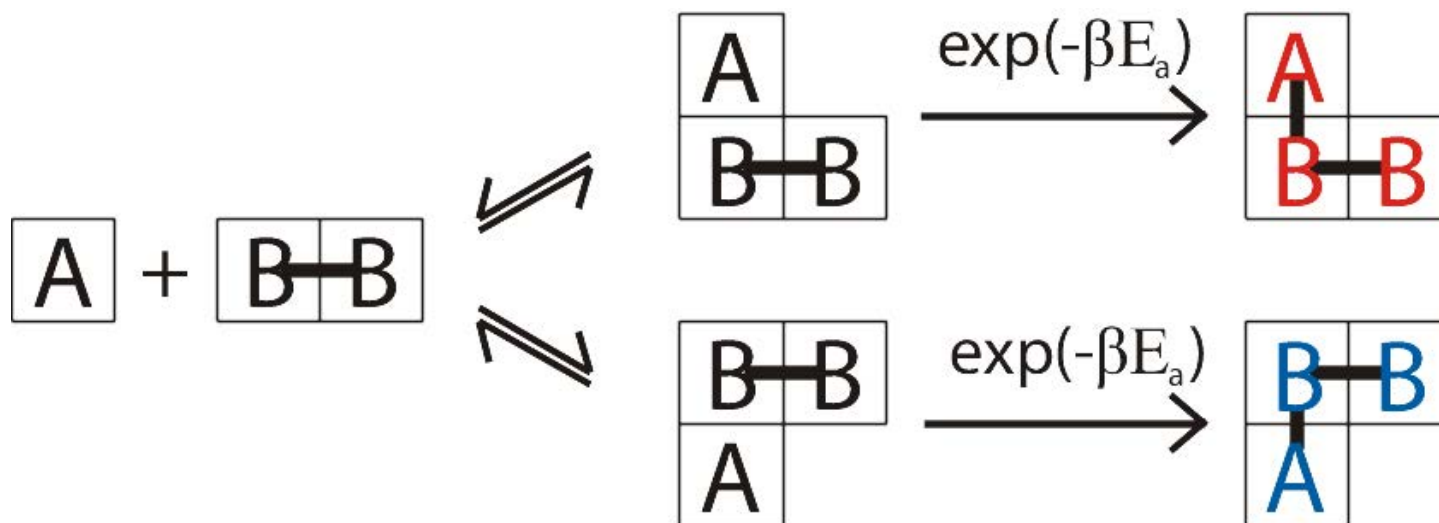
POSSIBLE MECHANISMS

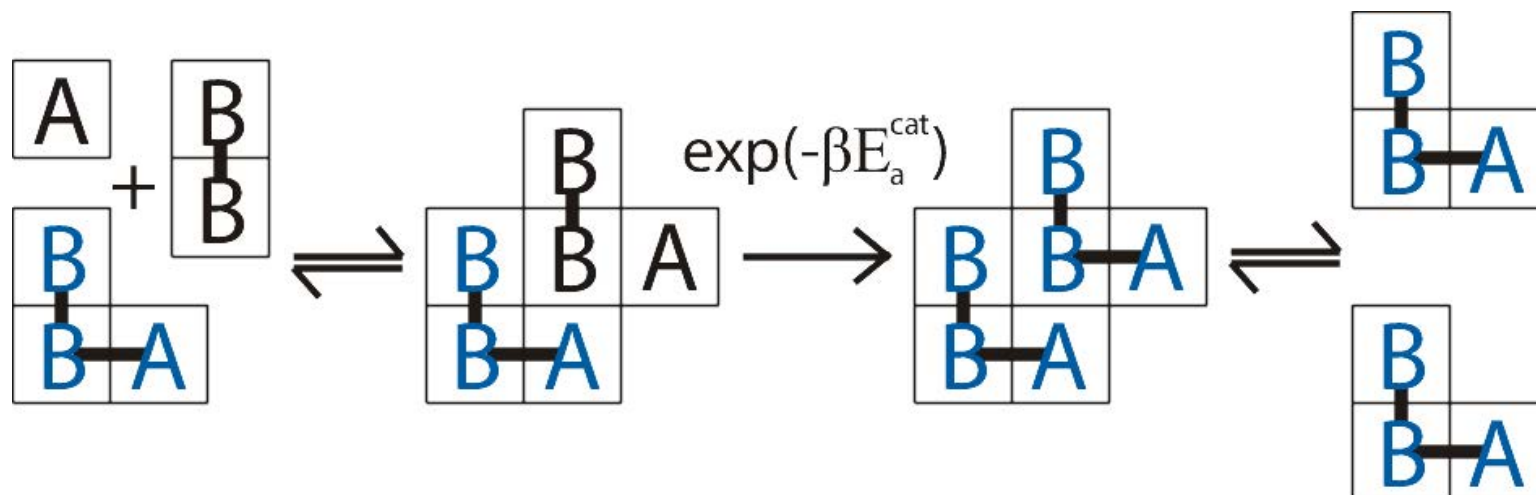
- (1) Parity-violating weak interactions
- (2) Illumination with circularly polarized light
- (3) D,L phase diagram characteristics:
enantiomeric excess amplification resulting
from off-symmetry eutectic pairs
- (4) Mechanically disturbed crystallization with slow
liquid-phase D,L interconversion, and "Ostwald
ripening"
- (5) Liquid-phase chemical kinetics with autocatalysis
and inhibition

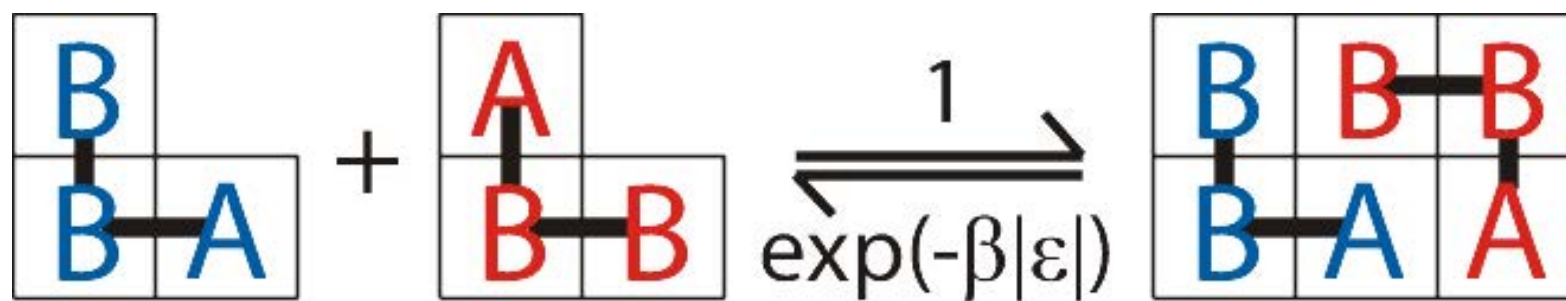
TWO-DIMENSIONAL LATTICE MODEL

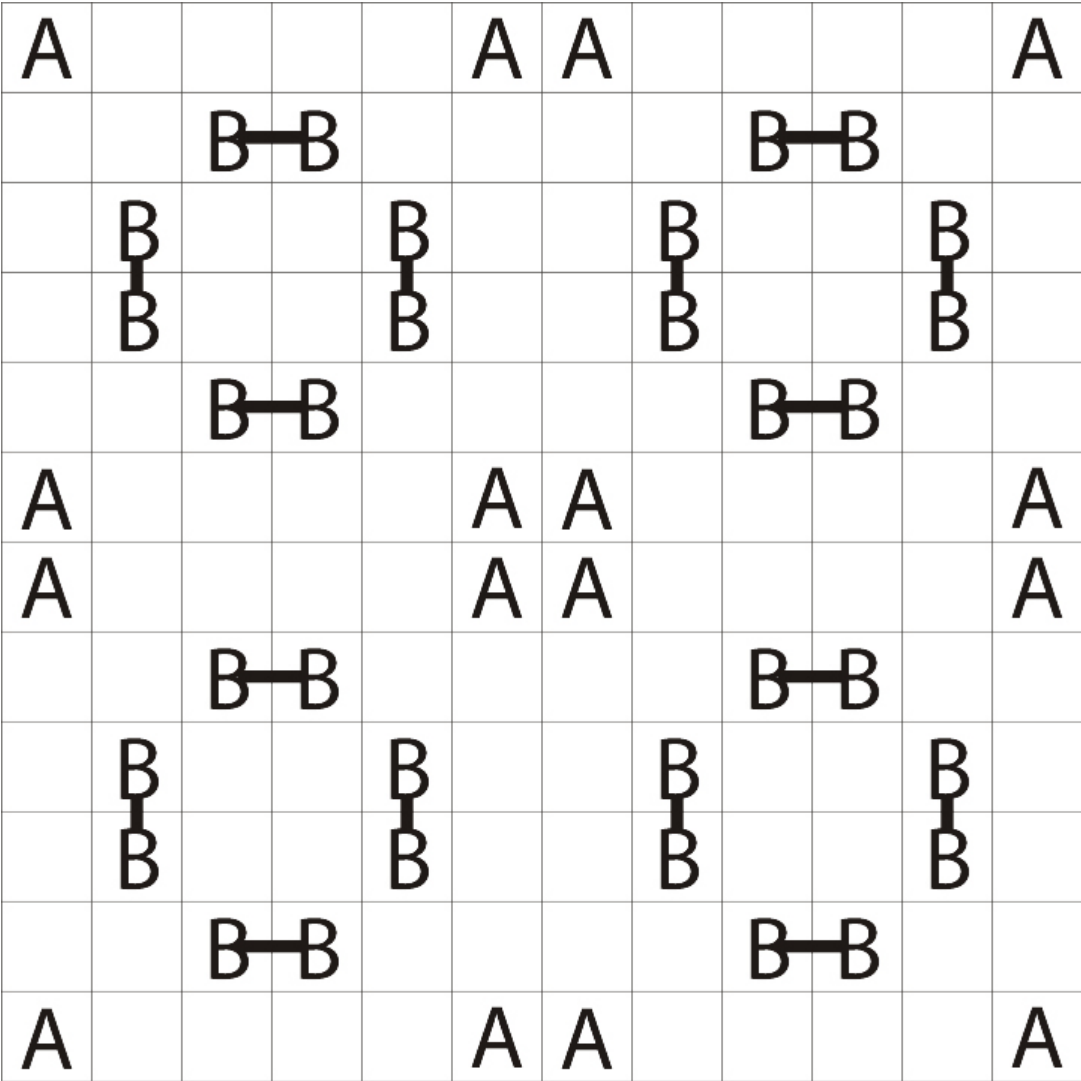
BACK

- Square lattice, two achiral reactants A and B—B
- Rigid chiral reaction products $\begin{array}{c} \text{B—B} \\ | \\ \text{A} \end{array}$ and $\begin{array}{c} \text{B—B} \\ | \\ \text{A} \end{array}$
- "Empty" sites represent inert solvent
- Random nearest-neighbor diffusive jumps before and after reaction





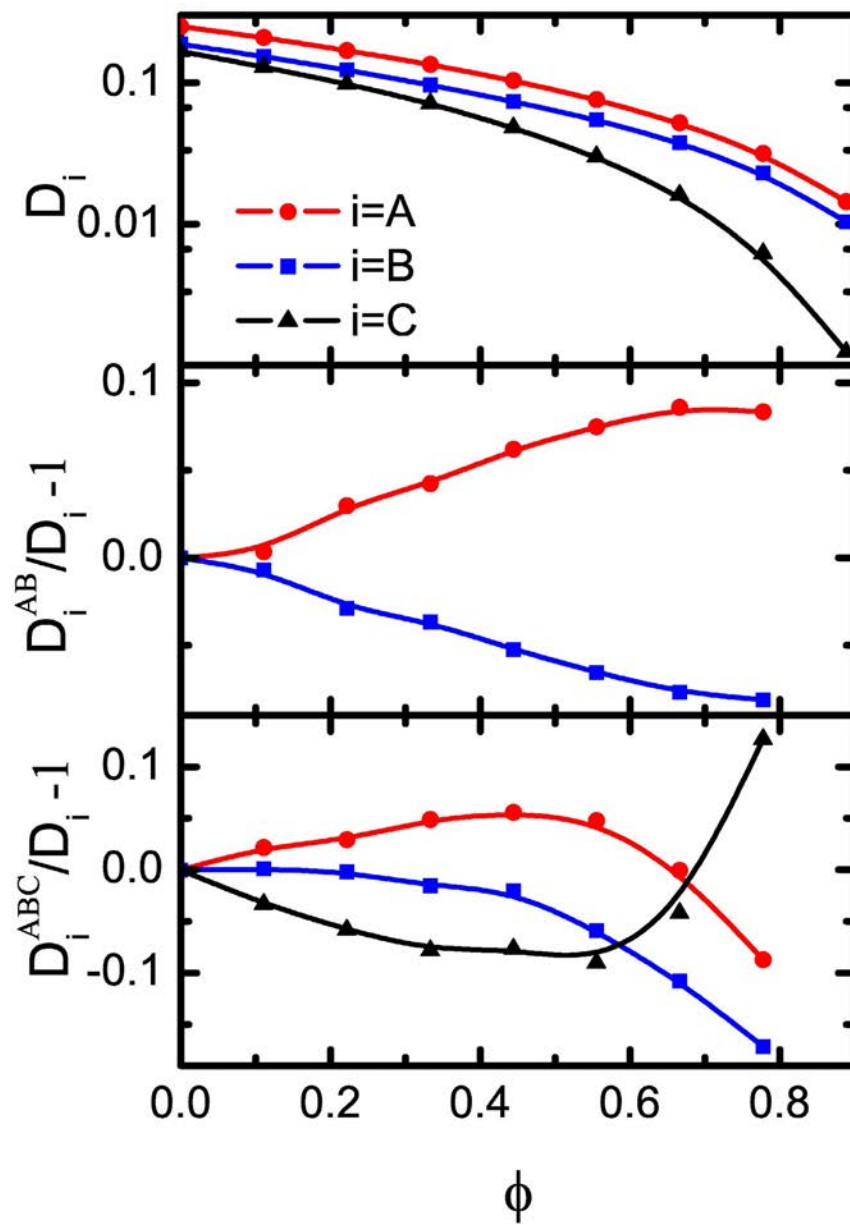


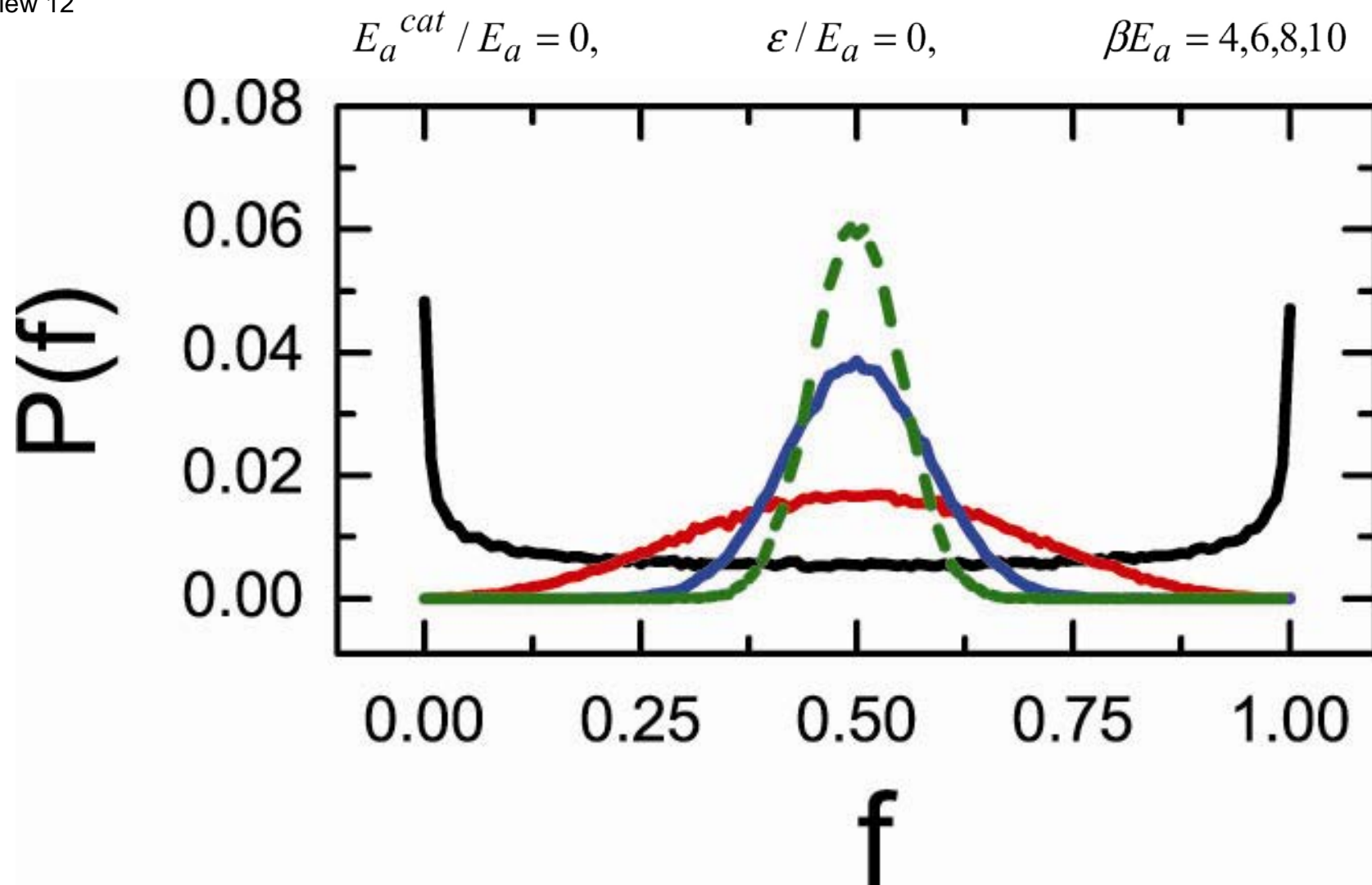


MONTE CARLO SIMULATION DETAILS

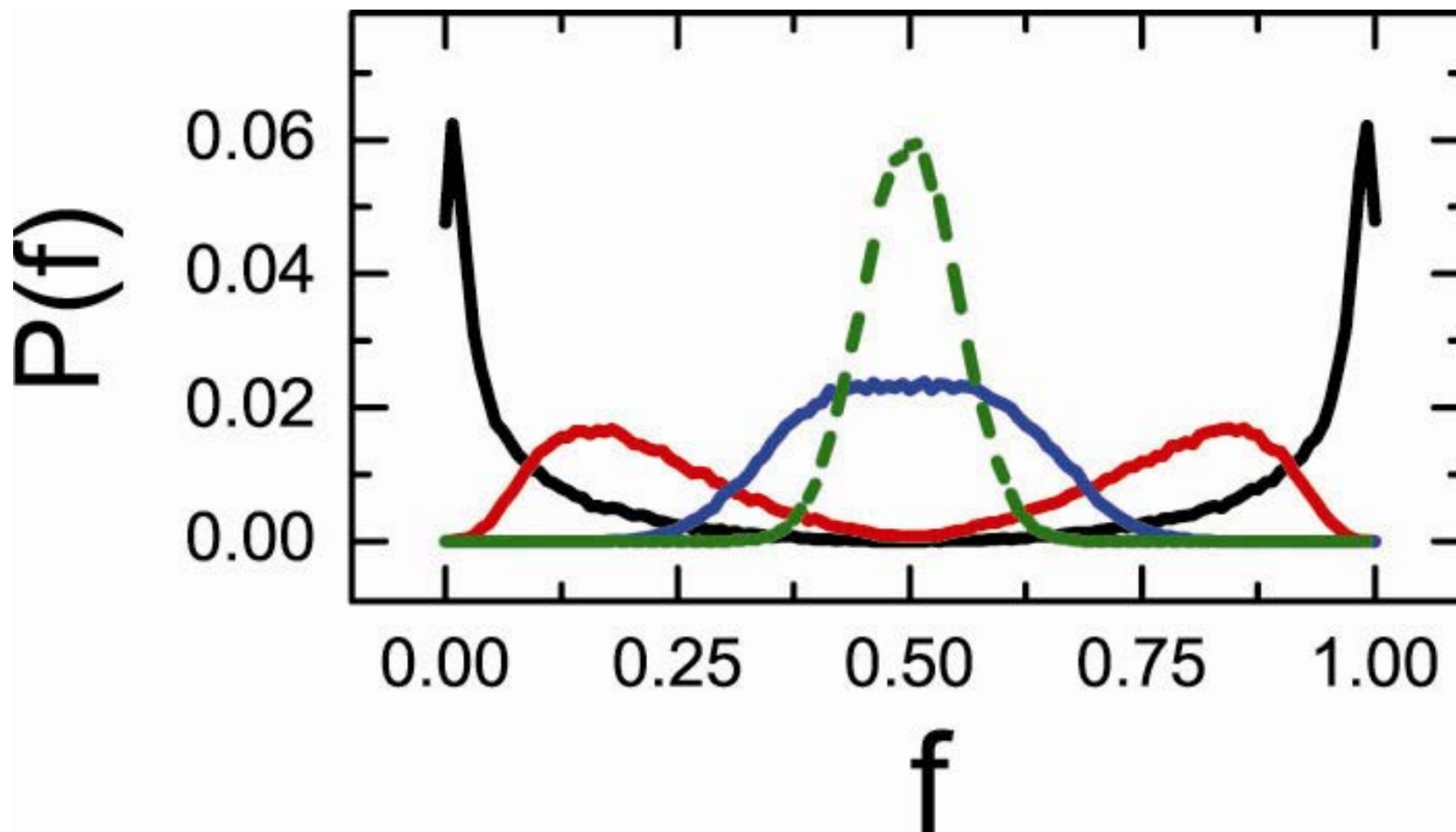
- Simulation runs performed on 36×36 and 90×90 square lattices with periodic boundary conditions, equal numbers of A and B–B reactants.
- Particles visited randomly. At each visit a chemical reaction or a diffusive jump (translational, rotational) is attempted.
- After each particle visit, time is advanced by $\Delta t = \tau / N$ (N = no. of rigid particles, τ = ave. time between visits to a given particle).
- MC run terminated when 80% of reactants have been consumed.
- 10^4 to 10^5 equivalent runs performed to determine the symmetric distribution function of the final enantiomer mole fraction:

$$0 \leq f = \frac{(D)}{(D) + (L)} \leq 1 \quad .$$





$$E_a^{cat} / E_a = 0, \quad \varepsilon / E_a = -10, \quad \beta E_a = 4, 6, 8, 10$$



SKEWNESS MEASURE FOR ENANTIOMORPHIC EXCESS

- Definition of enantiomorph excess:

$$e = |2f - 1|, \quad 0 \leq e \leq 1.$$

- Distribution of enantiomorph excess $\hat{P}(e)$ with moments:

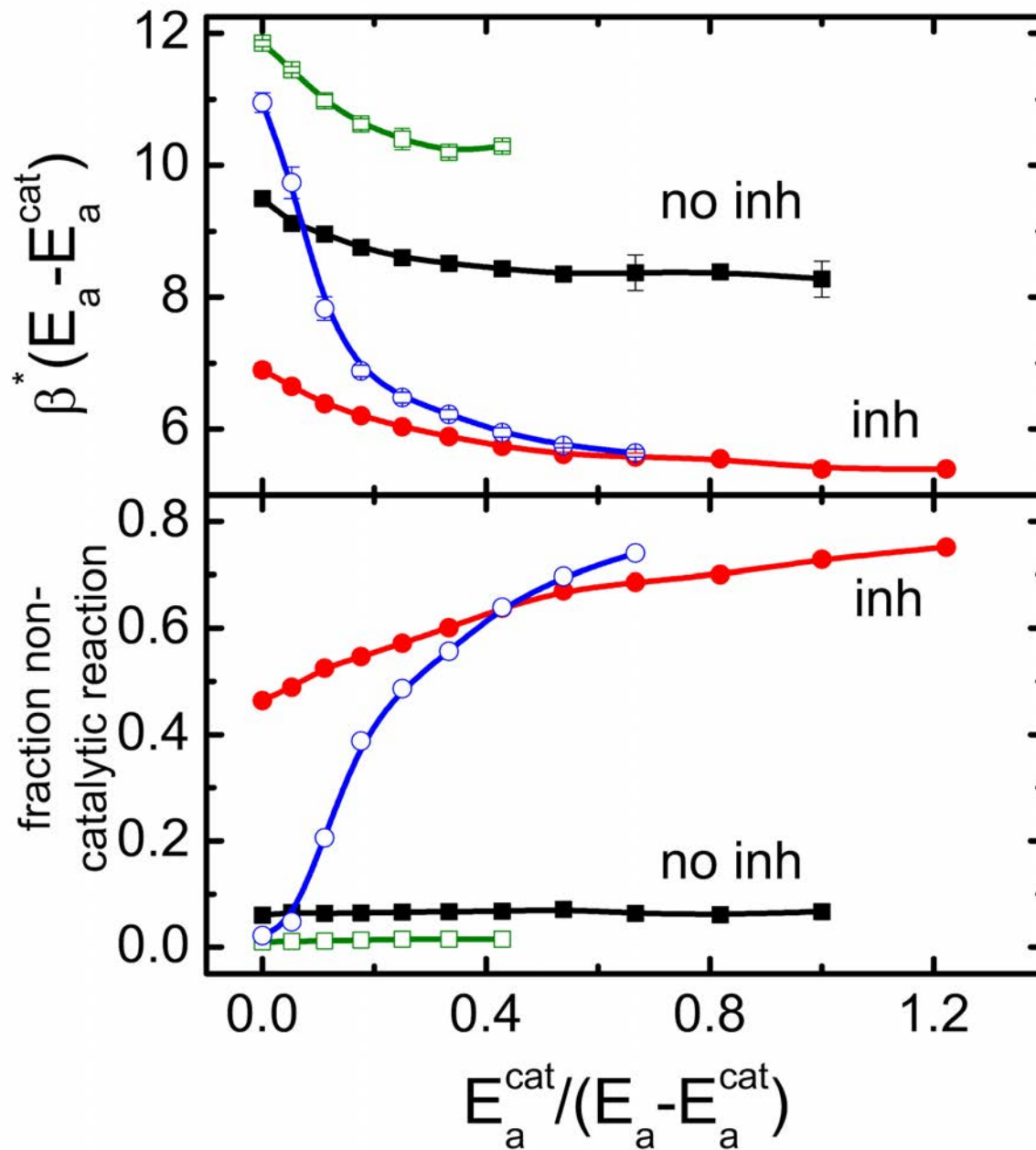
$$\langle e \rangle = \int_0^1 e \hat{P}(e) de, \quad m_2 = \langle [e - \langle e \rangle]^2 \rangle,$$

$$m_3 = \langle [e - \langle e \rangle]^3 \rangle.$$

- Skewness definition:

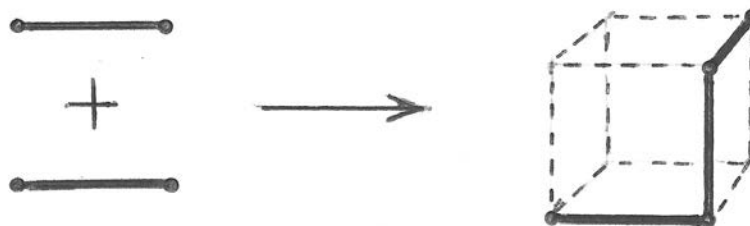
$$g = \frac{m_3}{(m_2)^{3/2}}.$$

- For chiral symmetry-unbroken cases [unimodal $P(f)$], $g > 0$.
For chiral symmetry broken cases [bimodal $P(f)$], $g < 0$.
- Symmetry-breaking "phase transition" identified with $g = 0$.

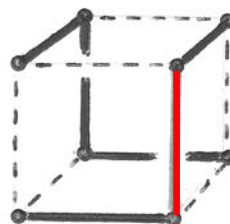


D=3 EXTENSION: THE SIMPLE CUBIC LATTICE

- Two neighboring dimers react, forming nonlinear chiral tetramer:



- Autocatalysis cluster occupies all 8 cube vertices:



- Scalar triple product of bond vectors distinguishes enantiomers:

$$(\mathbf{r}_{12} \times \mathbf{r}_{23} \cdot \mathbf{r}_{34}) / l^3 = \pm 1$$

CONCLUDING REMARKS

- Although not present in the model investigated, hydrodynamic convection or mechanical stirring would magnify the effectiveness of inhibition.
- Conversion of lattice model to a continuum model is feasible, but technically complicated.
- Chemical reaction reversibility can be included. One possible aspect would be to allow two molecules of the same chirality to bind to (*i.e.*, "gang up on") one molecule of the opposite chirality and cause it to revert to its unbonded precursor reactants.